

THE MELT\SHRINK EFFECT OF LOW DENSITY THERMOPLASTICS INSULATES: CONE CALORIMETER TESTS

Qiang XU¹, Cong JIN², Jordan HRISTOV³, Greg GRIFFIN⁴, Yong JIANG^{5*}

¹School of Mechanical Engineering, Nanjing University of Science and Technology, Nanjing 210014, China

²School of Computer Science and Technology, Nanjing University of Science and Technology, Nanjing 210014, China

Jordan HRISTOV⁵, Department of Chemical Engineering, University of Chemical Technology and Metallurgy, Sofia 1756, 8 Kliment Ohridsky, Blvd., Bulgaria

⁴School of Civil, Environmental and Chemical Engineering, University of RMIT, Melbourne, Victoria 3001, Australia

⁵State Key Laboratory of Fire Science, University of Science and Technology of China, Hefei 230026, China

- Author for correspondence: yjjiang@ustc.edu.cn, Tel: 86 551 63607827

Abstract

The melt\shrink effects on the fire behaviour of low-density thermoplastic foam have been studied in a cone calorimeter. The experiments have been performed with four samples of expanded polystyrene (EPS) foams having different thicknesses and two extruded polystyrene (XPS) foams. Decrease in surface area and increase in density, characterizing the melt\shrink effect have been measured at different incident heat fluxes. Three of these foams tested have been also examined by burning tests at an incident heat flux of 50kW m^{-2} . It was assessed that the fire behavior predictions based the current literature models provided incorrect results if the cone test results were applied directly. However, the correct models provided adequate results when the initial burning area and the density of the molten foam were used to correct the initial cone calorimeter data. This communication refers to the fact that both the effective burning area and the density of the molten foam affect the cone calorimeter data, which requires consequent corrections to attain adequate predictions of models about the materials fire behaviour.

Keywords: melt\shrink behaviour, cone calorimeter, flammability, thermoplastic foam, fire behavior

1 Introduction

Low density thermoplastic foams are widely encountered in soft furnishings and construction industries. The poor flammability performance of thermoplastic-based products causes fire to be a significant contributor to annual fire losses. An illegal fireworks show, for example, has ignited a thermoplastic insulation and the resultant fire gutted a 30-story building in Beijing's Central Business District on Feb. 9, 2009, China. One fireman died, while six firemen and two construction workers were injured. The cost of the fire was estimated at more than 23.44 million U.S. dollars. In this context, the fire at the Kiss nightclub in the south Brazil's college town of Santa Maria killed 235

people on Jan. 27, 2013, and it appears to have started when the band lit a flare that ignited the flammable sound-proofing foam boards. The fire safety performance of thermoplastic foam raises great concerns.

In NIST “Flammability of Thermoplastic Materials” project [1], characterizing melt/drip effects is one of the key goals of designing and assembling the necessary apparatus for developing bench scale flammability measurement methods. The melting effect is especially important for characterizing flammability of thermoplastic foams. It causes the foam to shrink and drip during a test; therefore the density and surface area exposed to the heat flux undergoes a significant change in bench scale tests.

Numerical and experimental tests have been performed in melt burning research [2, 3] Moreover, experimental research on the melt/drip effects have been carried out at different scales by standard and self-designed facilities [4-7]. In these experiments, specimens from 8 commercial products (all densities are more than 550kg m^{-3}), have been tested with UL94 in vertical burning test conditions [4]: mass loss rate, first drop mass and diameter, first dripping time were used to describe the melt/drip effect in the experiment. Thermal stabilities of another eight thermoplastic polymers have been studied by bench scale UL94 test and micro scale thermogravimetric (TG) test regarding the ignition mechanism of melting polymers [5,6].

In prediction of fire behaviour of materials both modeling and experiments need to be performed together providing mutual information for improving the fire tests. There is a variety of experiments in this direction, still sporadic to some extent, but providing step-by-step enough amount of data about the fire behaviour of thermoplastics in fire, especially the foams. In this context, simulation of polymer burning under UL94 vertical test conditions based on mass loss rate to investigate the change in density to the predicted have been carried out [7]. As a supporting technique, TG experiments have been used to estimate the onset of melting and then to provide adequate results for modeling both the melting and pyrolysis stages [8]. Increasing in the scale of the experiments resulted (with ISO 9705) to study polymer melt flow behavior and subsequent pool fire [9] in room scale tests; the interaction between a vertical polymer sheet fire and the induced pool fire were studied. Other factors, regression, char layer and fire spread, which influence the burning behavior of polymer have also been studied by [10-12].

A T-shape trough to study the flowing behavior of melting thermoplastics [13], and large scale burning tests were carried out for thermoplastics of different thickness [14]. A methodology to record the real-time melt and burning/dripping behavior of thermoplastics quantitatively in an electric furnace heated by connective heat flow have been developed [15]. Multi-scale test was also adopt to study the fire behavior of EPS foam [16].

In fact, it is difficult to characterize the fire behavior of foams [17] due to melt/drip effect of samples when tested. Melt/drip effects not only change the ignition mechanism of thermoplastics resulting in ignition time scatter, but also raise the uncertainties in heat release rate (HRR) measurements in cone calorimetric tests. HRR is an essential parameter in fire testing and flammability assessment, especially for performance based fire safety design in which HRR of materials is used for fires design in enclosures. Many software packages use HRR as input data for full scale fire predictions and material or product evaluation in light of fire behaviour. Thus, reliable HRR data are essential pool of information for correct evaluation materials and prediction their fire behaviors.

Cone calorimeter has been widely used in evaluating fire behavior of polymers in fire safety engineering. When the flammability of low density thermoplastic a horizontal placement of the sample is measured by the cone calorimeter and, the material can melt and shrink in the sample holder; the sample cannot drip but it may shrink during the melting stage; thus melt\drip effects is changed to melt\shrink effect. This is quite different from the test material which is liquid [18] or solid [19, 20] can hold its shape or burning area. If the sample is shrinking, then the exposed area to incident heat flux should be significantly smaller than the nominal exposure area used to calculate the heat release rate per square meter. It was found that the sample size can influence the cone test results [21]: the ignition of smaller PU adhesive samples was attributed to an enhanced mixing of volatiles and oxygen as a result of an increased distance between the conical heater and the sample surface. This interpretation refers an effective area of sample which has to be determined in order to perform an adequate ignition procedure as well as for the consequent calculations of heat release rate per area. As a support of these comments, an incorrect heat release rate obtained from a cone calorimeter test with a nominal sample surface (for example 0.008848m^2) as burning area would cause the fire behavior predictions invalid if the current models would be directly applied.

As examples of direct application of the current model predictions to cone calorimeter data obtained with melting materials we have to mention some research carried out. The fire behavior of sandwich panels [20] using expanded polystyrene core, expanded polystyrene cores was classified as FO-category 4 by Östman's model [23] and Hansen's model [24] from cone calorimeter tests using 50 kW m^{-2} incident heat flux. Thus an ISO 9705 room fire test on a room lined with EPS panels (without skins) is predicted to reach flashover before 2 min after the beginning of the test. Six out of eight tests reached flashover, all the flashover happened after 5min, only two of them reached flashover before 10min. These models are not able to be applied to data about composite materials and cannot predict the time to flashover for sandwich panels [22].

Heating and ignition tests were conducted in our research to study the melt\shrink effect in cone calorimetric tests. Density and surface area changes are measured for test samples at different incident heat fluxes in heating tests. Ignition tests were carried out at 50 kW m^{-2} incident heat flux. Density and surface area of melt\shrink foams is used to correct the 50 kW m^{-2} results and input to fire behavior prediction models. The low density foams are classified by Östman's and Hansen's model using 50 kW m^{-2} test data directly and the corrected data. The difference of prediction results is analyzed. The main goal of this research is to deduce the correlation between melt\shrink effect and the heat release rate measurement and explore a method to use the test results in fire behavior prediction.

2 Test Descriptions

2.1 Test facilities

The tests were performed with the cone calorimeter in the State Key Laboratory of Fire Science, China, and this cone is in accordance with ISO 5660. All test specimens were wrapped in aluminium foil with the upper surface uncovered, put into a specimen-holder and exposed in the horizontal orientation. Specimens were packed to the appropriate test level height using Kaowool ceramic fiber. The specimen-holder's edge frame retains the specimen as allowed in the Standard. The edge frame reduces the test surface area to 0.008848 m^2 , and this is the area used in calculations. The nominal

exhaust system flow rate for all tests was $0.024 \text{ m}^3 \text{ s}^{-1}$. Prior to testing, a PMMA reference material was tested to ensure that all systems were working correctly.

2.2 Materials and tests arrangement

Six kinds of thermoplastic foams were tested in this research. Four of them were expanded polystyrene (EPS) foam panel, and two were extruded polystyrene (XPS) foam panel. These materials' parameters and labels are listed in Table 1, Photos of tested samples are shown in Fig.1.

Table 1. Materials used in the tests

| | EPS | EPS | EPS | EPS | XPS | XPS |
|-----------------------------|---------|----------|----------|----------|-----------|------------|
| $\rho_n / \text{kg m}^{-3}$ | 6.5 | 5.3 | 7.8 | 8.2 | 52.6 | 37.8 |
| Thickness /mm | 8 | 12 | 18 | 48 | 20 | 18 |
| Color | White | White | White | white | red | Grey |
| Material label | EPS_8 | EPS_12 | EPS_18 | EPS_48 | XPS_red | XPS_grey |
| Test label | EPS_8_* | EPS_12_* | EPS_18_* | EPS_48_* | XPS_red_* | XPS_grey_* |

* Incident heat flux in cone test, for example, EPS_8_25 is the EPS specimen with the thickness of 8mm at the incident heat flux of 25 kW m^{-2} .

The tests were conducted in two stages. In the first stage, burning tests were conducted for EPS_48, XPS_red, and XPS_grey at incident heat flux of 25, 35, 50 kW m^{-2} . Triplicate specimens of each material were tested at each incident heat flux, except for XPS_red and XPS_grey at 50 kW m^{-2} , only one test was conducted for each of them.

In the second stage, only heating tests were conducted. Three EPS panels with thickness of 8, 12, and 18mm were heated with the cone under incident heat flux of 25, 35, 50 kW m^{-2} for 10 to 15 seconds. Triplicate specimens of each material were tested under each incident heat flux. Heating tests were also conducted for EPS_48, XPS_red, and XPS_grey under incident heat flux of 25, 35, 50 kW m^{-2} , the heating procedure stopped 10 to 20 seconds before the mean ignition time for each materials - as obtained from first stage tests. Triplicate specimens of each material were also tested under each incident heat flux. The heating times chosen for EPS_48 are 90, 60, and 40 seconds, for XPS_red are 80, 50, and 30seconds, for XPS_grey are 110, 40 and 10 seconds.

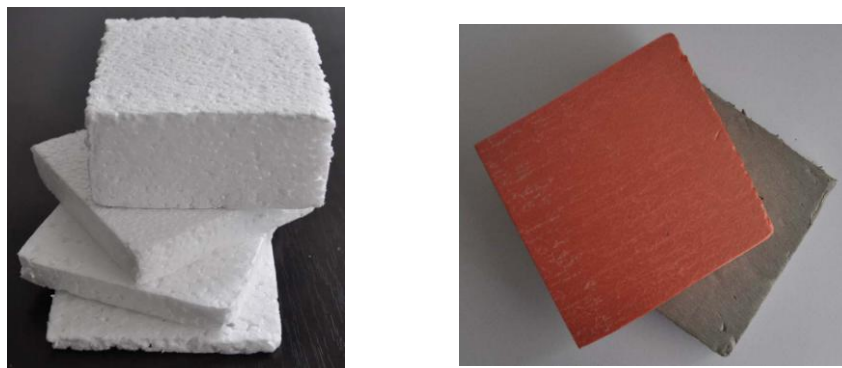


Fig.1 Prepared specimens for cone tests. Left: EPS , Right: XPS

3 Test results

3.1 Melt\shrink effect of foams

The original remains of second stage tests are shown in Fig.2. The melt\shrink effect is clear for all the tested thermoplastic foams.



Fig.2 Heating test remains

To quantify the effect, all remains are taken from the aluminium foil with their original shape and put on a 94mm×94mm blue (for EPS specimens) and white (for XPS specimens) paper to take photos. Processed photos are illustrated in Fig.3 and Fig.4. The reduced surface areas of the molten specimens are calculated and listed in Tabel.2 and 3. The volume of each residue was also measured, thus its density is calculated; these are also listed in Tabel.2 and 3. Incident heat flux has more influence on density than surface area.

With low nominal density and the lowest mass, EPS_8 specimens shrank to a very low effective surface area decrease to a very low level, see Tabel.2-1 and 2-2. For EPS specimens, the more nominal density and mass, the more effective surface area would be reached, see also Tabel.2-1 and 2-2.

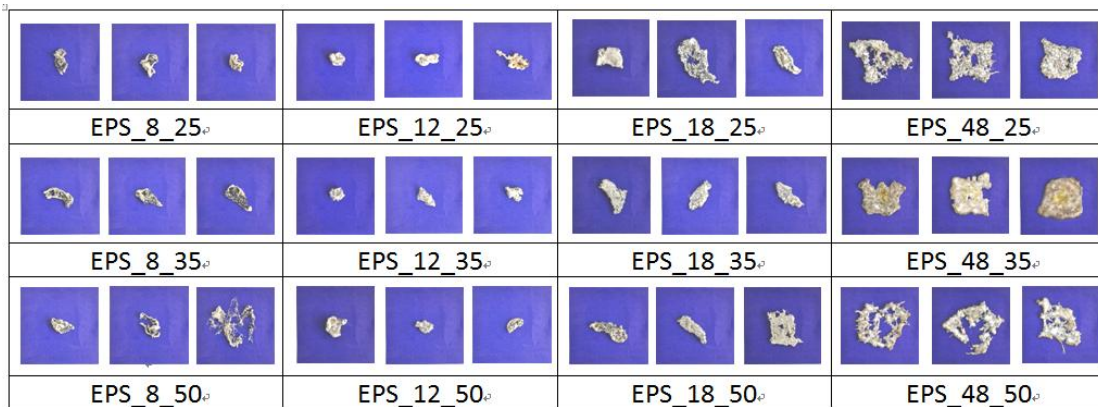


Fig.3 Processed images of EPS remains

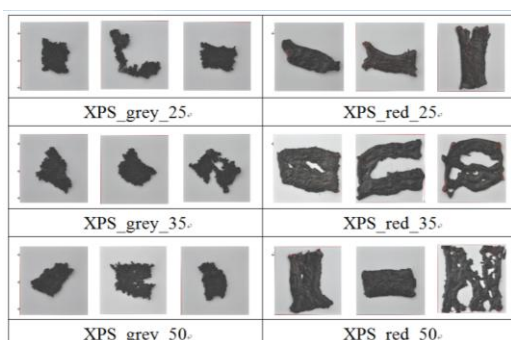


Fig.4 Processed images of XPS remains

Table 2-1. Area and density change of EPS specimens

| Incident heat flux /kW m ⁻² | EPS-8 | | | | | | EPS-12 | | | | | |
|--|------------------|----------------|--------------|---------------------------------|-------------------|------------------------------------|------------------|----------------|--------------|---------------------------------|-------------------|------------------------------------|
| | Specimen mass /g | Mass remain /g | Mass loss /g | A _e /mm ² | R _a /% | ρ _m /kg m ⁻³ | Specimen mass /g | Mass remain /g | Mass loss /g | A _e /mm ² | R _a /% | ρ _m /kg m ⁻³ |
| 25 | 0.52 | 0.51 | 0.01 | 250 | 2.83 | 217 | 0.63 | 0.61 | 0.02 | 381 | 4.30 | 231 |
| 25 | 0.51 | 0.49 | 0.02 | 293 | 3.31 | 203 | 0.64 | 0.61 | 0.03 | 311 | 3.51 | 252 |
| 25 | 0.52 | 0.50 | 0.02 | 246 | 2.78 | 208 | 0.61 | 0.60 | 0.01 | 231 | 2.61 | 249 |
| Mean | 0.52 | 0.50 | 0.02 | 263 | 2.97 | 209 | 0.63 | 0.61 | 0.02 | 307 | 3.47 | 244 |
| SD | 0.01 | 0.01 | 0.01 | 26 | 0.29 | 7 | 0.02 | 0.01 | 0.01 | 75 | 0.85 | 11 |
| 35 | 0.51 | 0.50 | 0.01 | 388 | 4.39 | 238 | 0.61 | 0.59 | 0.02 | 181 | 2.05 | 298 |
| 35 | 0.53 | 0.50 | 0.03 | 326 | 3.68 | 192 | 0.61 | 0.58 | 0.03 | 267 | 3.02 | 239 |
| 35 | 0.51 | 0.49 | 0.02 | 260 | 2.94 | 222 | 0.60 | 0.56 | 0.04 | 252 | 2.85 | 264 |
| Mean | 0.52 | 0.50 | 0.02 | 325 | 3.67 | 217 | 0.61 | 0.58 | 0.03 | 234 | 2.64 | 267 |
| SD | 0.01 | 0.01 | 0.01 | 64 | 0.73 | 23 | 0.01 | 0.02 | 0.01 | 46 | 0.52 | 30 |
| 50 | 0.52 | 0.50 | 0.02 | 312 | 3.53 | 248 | 0.62 | 0.59 | 0.03 | 388 | 4.39 | 268 |
| 50 | 0.52 | 0.49 | 0.03 | 265 | 2.99 | 245 | 0.63 | 0.58 | 0.05 | 221 | 2.50 | 297 |
| 50 | 0.55 | 0.50 | 0.05 | 910 | 10.28 | 166 | 0.65 | 0.60 | 0.05 | 181 | 2.05 | 302 |
| Mean | 0.53 | 0.50 | 0.03 | 496 | 5.60 | 220 | 0.63 | 0.59 | 0.04 | 264 | 2.98 | 289 |
| SD | 0.02 | 0.01 | 0.02 | 359 | 4.06 | 47 | 0.02 | 0.01 | 0.01 | 110 | 1.24 | 18 |

Table 2-2. Area and density change of EPS specimens

| Incident heat flux /kW m ⁻² | EPS-18 | | | | | | EPS-48 | | | | | |
|--|------------------|----------------|--------------|---------------------------------|-------------------|------------------------------------|------------------|----------------|--------------|---------------------------------|-------------------|------------------------------------|
| | Specimen mass /g | Mass remain /g | Mass loss /g | A _e /mm ² | R _a /% | ρ _m /kg m ⁻³ | Specimen mass /g | Mass remain /g | Mass loss /g | A _e /mm ² | R _a /% | ρ _m /kg m ⁻³ |
| 25 | 1.41 | 1.38 | 0.03 | 611 | 6.91 | 403 | 3.92 | 3.87 | 0.05 | 1787 | 20.20 | 719 |
| 25 | 1.44 | 1.43 | 0.01 | 1186 | 13.40 | 450 | 3.83 | 3.80 | 0.03 | 2073 | 23.43 | 639 |
| 25 | 1.45 | 1.61 | 0.04 | 534 | 6.04 | 468 | 3.95 | 3.91 | 0.04 | 1820 | 20.58 | 680 |
| Mean | 1.43 | 1.47 | 0.03 | 777 | 8.78 | 440 | 3.90 | 3.86 | 0.04 | 1894 | 21.40 | 679 |
| SD | 0.02 | 0.12 | 0.02 | 356 | 4.02 | 34 | 0.06 | 0.06 | 0.01 | 156 | 1.77 | 40 |
| 35 | 1.44 | 1.39 | 0.05 | 635 | 7.18 | 411 | 3.93 | 3.89 | 0.04 | 1831 | 20.69 | 850 |
| 35 | 1.44 | 1.41 | 0.03 | 580 | 6.56 | 463 | 4.03 | 3.98 | 0.05 | 2087 | 23.59 | 781 |
| 35 | 1.46 | 1.40 | 0.06 | 488 | 5.51 | 487 | 4.06 | 3.99 | 0.07 | 2271 | 25.67 | 776 |
| Mean | 1.45 | 1.40 | 0.05 | 568 | 6.42 | 454 | 4.01 | 3.96 | 0.05 | 2063 | 23.32 | 802 |
| SD | 0.01 | 0.01 | 0.02 | 75 | 0.84 | 39 | 0.07 | 0.06 | 0.02 | 221 | 2.50 | 41 |
| 50 | 1.49 | 1.43 | 0.06 | 489 | 5.53 | 514 | 3.64 | 3.58 | 0.06 | 2126 | 24.03 | 661 |
| 50 | 1.46 | 1.41 | 0.05 | 477 | 5.39 | 487 | 3.74 | 3.67 | 0.07 | 1932 | 21.83 | 779 |
| 50 | 1.45 | 1.41 | 0.04 | 1103 | 12.47 | 509 | 4.05 | 3.99 | 0.06 | 2147 | 24.26 | 789 |
| Mean | 1.47 | 1.42 | 0.05 | 670 | 7.80 | 503 | 3.81 | 3.75 | 0.06 | 2068 | 23.37 | 743 |
| SD | 0.02 | 0.01 | 0.01 | 358 | 4.05 | 14 | 0.21 | 0.22 | 0.01 | 119 | 1.34 | 71 |

Table 3. Area and density change of XPS specimens

| Incident heat flux /kW m ⁻² | XPS_red | | | | | | XPS_grey | | | | | |
|--|------------------|----------------|--------------|---------------------------------|-------------------|------------------------------------|------------------|----------------|--------------|---------------------------------|-------------------|------------------------------------|
| | Specimen mass /g | Mass remain /g | Mass loss /g | A _e /mm ² | R _a /% | ρ _m /kg m ⁻³ | Specimen mass /g | Mass remain /g | Mass loss /g | A _e /mm ² | R _a /% | ρ _m /kg m ⁻³ |
| 25 | 10.32 | 9.83 | 0.49 | 3066 | 34.66 | 520 | 6.34 | 6.28 | 0.06 | 1497 | 16.93 | 569 |
| 25 | 10.11 | 9.84 | 0.27 | 2131 | 24.08 | 509 | 5.92 | 5.90 | 0.02 | 1701 | 19.23 | 651 |
| 25 | 10.31 | 9.89 | 0.42 | 2074 | 23.44 | 588 | 5.76 | 5.73 | 0.03 | 1555 | 17.57 | 705 |
| Mean | 10.25 | 9.85 | 0.39 | 2424 | 27.39 | 539 | 6.01 | 5.97 | 0.04 | 1585 | 17.91 | 642 |
| SD | 0.12 | 0.03 | 0.11 | 558 | 6.30 | 43 | 0.30 | 0.28 | 0.02 | 105 | 1.19 | 69 |
| 35 | 10.73 | 10.16 | 0.57 | 4342 | 49.07 | 534 | 6.29 | 6.26 | 0.03 | 1725 | 19.50 | 706 |
| 35 | 11.31 | 11.01 | 0.30 | 4702 | 53.14 | 782 | 6.32 | 6.27 | 0.05 | 1594 | 18.01 | 789 |
| 35 | 11.11 | 10.67 | 0.45 | 4322 | 48.85 | 734 | 6.26 | 6.19 | 0.07 | 2101 | 23.74 | 600 |
| Mean | 11.05 | 10.67 | 0.44 | 4455 | 50.35 | 683 | 6.29 | 6.24 | 0.05 | 1807 | 20.42 | 698 |
| SD | 0.30 | 0.45 | 0.14 | 214 | 2.42 | 131 | 0.03 | 0.044 | 0.02 | 263 | 2.97 | 95 |
| 50 | 10.55 | 10.13 | 0.42 | 3730 | 42.16 | 733 | 6.01 | 5.95 | 0.06 | 1602 | 18.10 | 788 |
| 50 | 10.09 | 9.63 | 0.46 | 2642 | 29.86 | 911 | 5.95 | 5.93 | 0.02 | 2175 | 24.58 | 801 |
| 50 | 10.13 | 9.51 | 0.62 | 5400 | 61.03 | 839 | 5.90 | 5.79 | 0.11 | 1444 | 16.32 | 826 |
| Mean | 10.26 | 9.76 | 0.50 | 3924 | 44.35 | 828 | 5.95 | 5.89 | 0.06 | 1740 | 19.67 | 805 |
| SD | 0.26 | 0.33 | 0.11 | 1389 | 15.70 | 90 | 0.06 | 0.09 | 0.05 | 385 | 4.35 | 19 |

3.2 Influence on flammability prediction

In the second stage, burning tests were conducted for EPS_48, XPS_red, and XPS_grey at incident heat flux of 50 kW m⁻². The results are illustrated in Fig.5.

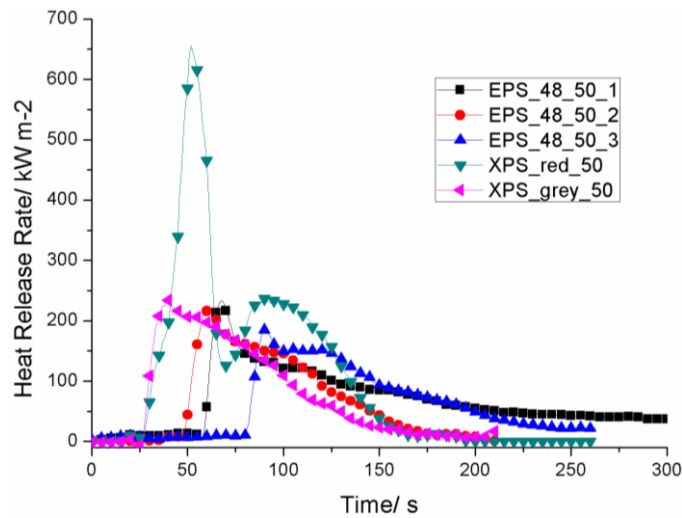


Fig.5 Heat release rate of at incident heat flux of 50 kW m⁻²

The cone calorimeter results of these thermoplastics from tests at 50 kW m⁻² are used as input data to Östman's [23] empirical linear regression model and Hansen's [24] multiple discriminant function analysis model to predict the FO-category in the ISO9705 room corner test. The FO-category is determined by application of the following set of rules:

- * FO-category 1: products not reaching flashover during 1200 seconds of testing time
- * FO-category 2: 600 seconds ≤ t_{FO} < 1200 seconds
- * FO-category 3: 120 seconds ≤ t_{FO} < 600 seconds
- * FO-category 4: t_{FO} < 120 seconds

The Östman's regression model[23] is expressed in the following equation

$$t_{FO} = 0.07 \frac{t_{ig}^{0.25} \rho^{1.7}}{THR_{300}^{1.3}} + 60 \quad (1)$$

where t_{FO} is the time to flashover in the room corner test, t_{ig} is the time to ignition in the cone calorimeter at 50 kW m⁻², THR₃₀₀ is the total heat release during 300s after ignition at 50 kW m⁻² and ρ is the mean density. All of these three foams are classified to FO-category 4, which would reach flashover in ISO room test within 120 seconds, see Table 4.

In Hansen's model [24], the four classification functions that are expressed as follows:

$$F_{FO1} = 0.01789z_1 - 0.06057z_2 + 0.971z_3 - 7.910 \quad (2)$$

$$F_{FO2} = 0.01492z_1 + 0.03354z_2 + 1.877z_3 - 7.418 \quad (3)$$

$$F_{FO3} = 0.008589z_1 + 0.409z_2 + 2.721z_3 - 13.406 \quad (4)$$

$$F_{FO4} = 0.0000256z_1 + 0.347z_2 + 3.621z_3 - 9.215 \quad (5)$$

The selected parameters were

* z₁=ρ /kg m⁻³=density of samples

* z₂=THR₃₀₀ /MJ m⁻²=total heat release during 300 seconds after apparent time to ignition.

* z₃=ln(FIGRA_{cc}) where FIGRA_{cc} is the maximum value of the ratio between HRR and time when HRR was measured.

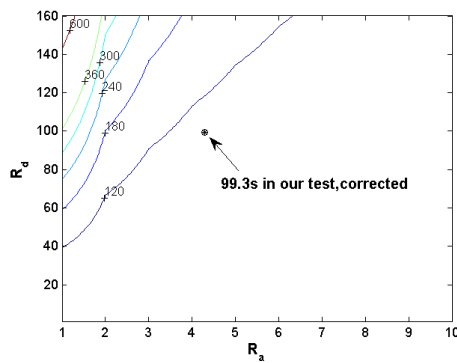
The parameter values and calculated results are also listed in Tabel.4. All F_{FO4} give the largest value of the four functions, the foams can be determined as a member of FO-category 4, which would reach flashover in ISO9705 test within 120 seconds; they are the same as the results from Östman's model. The values of all t_{fo} are all close to 60 seconds.

Table 4. Classification of results based on original 50 kW m⁻² test data

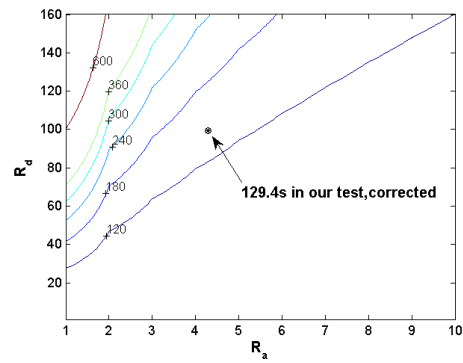
| | EPS_48_50-1 | EPS_48_50_2 | EPS_48_50_3 | XPS_red_50 | XPS_grey_50 |
|---------------------------------------|--------------|--------------|--------------|--------------|--------------|
| t _{ig} /s | 45 | 34 | 68 | 45 | 23 |
| z1-ρ _f /kg m ⁻³ | 8.2 | 8.2 | 8.2 | 52.6 | 37.8 |
| z2-THR300 /MJ m ⁻² | 21.17 | 12.96 | 14.72 | 27.29 | 16.14 |
| z3-ln(FIGRA _{cc}) | 1.23 | 1.31 | 0.715 | 2.54 | 1.77 |
| t _{FO} /s | 60.12 | 60.21 | 60.21 | 62.08 | 61.98 |
| F _{FO1} | -7.8523 | -7.2774 | -7.9617 | -6.1556 | -6.4927 |
| F _{FO2} | -4.2778 | -4.4030 | -5.4608 | -0.9503 | -2.9904 |
| F _{FO3} | -1.3307 | -4.4709 | -5.3701 | 5.1187 | -1.6639 |

| | | | | | |
|-------------|---------------|---------------|----------------|---------------|---------------|
| F_{FO4} | 2.5850 | 0.0258 | -1.5179 | 9.4533 | 2.7957 |
| FO-category | 4 | 4 | 4 | 4 | 4 |

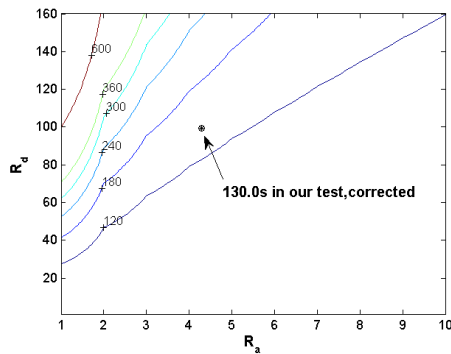
The effective area at 50 kW m^{-2} heat flux is used to correct $\text{THR}_{300}(z_2)$, and density of molten foam is used in Eq.1 and as z_1 in Hansen's model [24], the calculated results are listed in Tab.5. Three out of five results from Östman's model and all results from Hansen's model classify the foams as a member of FO-category 3. Obviously, in both Östman's and Hansen's models, the effective surface and density of molten play important role in the flammability prediction. Fig.6 shows the influence of R_a and R_d on t_{fo} with Östman's model.



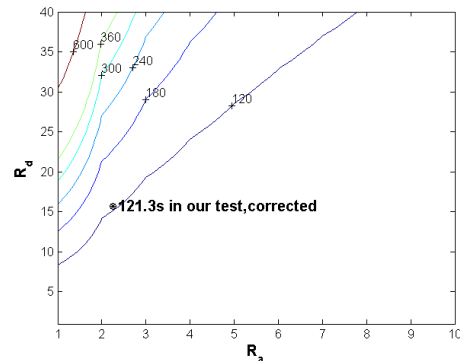
a) EPS_48_50_1 ($t_{ig}=45\text{s}$, $\text{THR}_{300}=21.17 \text{ MJ m}^{-2}$)



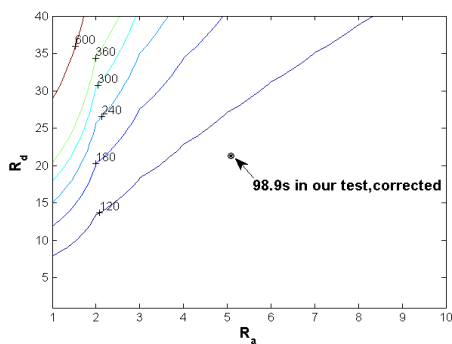
b) EPS_48_50_2 ($t_{ig}=34\text{s}$, $\text{THR}_{300}=12.96 \text{ MJ m}^{-2}$)



c) EPS_48_50_3 ($t_{ig}=68\text{s}$, $\text{THR}_{300}=14.72 \text{ MJ m}^{-2}$)



d) XPS_red_50 ($t_{ig}=45\text{s}$, $\text{THR}_{300}=27.29 \text{ MJ m}^{-2}$)



e) XPS_grey_50 ($t_{ig}=23\text{s}$, $\text{THR}_{300}=16.14 \text{ MJ m}^{-2}$)

Fig.6 The influence of area and density change on flashover time prediction (Östman's model)

Table 5. Classification of results based on corrected 50 kW m⁻² test data

| | EPS_48_50_1 | EPS_48_50_2 | EPS_48_50_3 | XPS_red_50 | XPS_grey_50 |
|----------------------------------|----------------|----------------|----------------|----------------|----------------|
| t_{ig} /s | 45 | 34 | 68 | 45 | 23 |
| $z1-\rho_m$ /kg m ⁻³ | 743 | 743 | 743 | 828 | 805 |
| $z2$ -THR300 /MJ m ⁻² | 90.6 | 55.5 | 63.0 | 61.5 | 82.1 |
| $z3$ -ln(FIGRA _{cc}) | 2.69 | 2.76 | 2.17 | 3.35 | 3.40 |
| t_{FO} /s | 99.3 | 129.4 | 130.0 | 138.3 | 103.3 |
| FO-category | 4 | 3 | 3 | 3 | 4 |
| F _{FO1} | 2.5066 | 4.7006 | 3.6734 | 6.4307 | 4.8201 |
| F _{FO2} | 11.7554 | 10.7096 | 9.8537 | 13.2864 | 13.7280 |
| F_{FO3} | 37.3505 | 23.1851 | 24.6472 | 27.9745 | 36.3384 |
| F _{FO4} | 31.9827 | 20.0565 | 20.5226 | 24.2770 | 31.6057 |
| FO-category | 3 | 3 | 3 | 3 | 3 |

4 Conclusions

The heat release rate per area of the foam depends on the effective burning area and the heat release of the molten pool. This would cause the estimation of the foam flammability more complicated than it is suggested by the existing in the literature models. Because of that, when the foam melts and shrinks, the effective burning area should be smaller than the standard burning area used in calculations of the heat release rate per area; this would cause a lower data of HRR. Shrunk foam would get less total heat flux from the cone heater; this would influence the ignition and subsequent burning process.

In cone calorimeter tests, both the effective burning area and the density of molten foam have significant effect on the results. The initial burning area could be used to correct the heat release rate per area of sample, but this is still a subject to a certain amount of uncertainty due to the burning area changing during the combustion process.

The current models used for prediction of fire behavior as well as the flammability classification methods are incorrect in case of low-density thermoplastics foams. In this context, even results based on corrected cone calorimeter test data need to be verified by full scale tests. In a real fire scenario, two key factors affect the fire behavior of the thermoplastic foams: the effective burning area and the flowing (or dripping) ability of the melts.

The fire behavior prediction model for low-density thermoplastics foams should include the effective burning area caused by melt\shrink effect, and the heat release rate of molten foam. For real fire scenarios the prediction of the flowing or dripping performance should be considered due to increase in the complexity in predicting the fire behavior. Moreover, it is necessary to study the melt\shrink performance of low-density thermoplastic foams when evaluating the flammability hazard.

Acknowledgements

This research is supported by the Natural Science Fund of China, No.51076065 and No. 51376093, the Open Funding from the State Key Laboratory of Fire Science in China, No. HZ2012-KF05. Authors wish to acknowledge Mr. Li Zhen for his help in cone tests.

Nomenclature

t_{fo} predicted flashover time, s

t_{ig} ignition time, s

ρ_n nominal density of foam, kg m^{-3}

ρ_m density of molten foam, kg m^{-3}

R_d ratio of density $\rho_m \rho_n^{-1}$

A_e effective area, mm^2

A_n nominal area, mm^2

R_a ratio of area, $A_n A_e^{-1}$

$PHRR$, peak heat release rate, kW m^{-2}

THR total heat release in specific time after ignition, MJ m^{-2}

References

- [1]. *** http://www.nist.gov/el/fire_protection/buildings/flammability_of_thermoplastic_materials.mht
- [2]. Marti J., Ryzhakov P., Idelsohn S., Onate E. Combined Eulerian-PFEM approach for analysis of polymers in fire situations, *Int. J. Numer. Meth. Eng.*, 92 (2012), 9, pp.782-801
- [3]. Onate E., Rossi R., Idelsohn S.R., Butler K.M.. Melting and spread of polymers in fire with the particle finite element method, *Int. J. Numer. Meth. Eng.*, 84 (2010), 8, pp.1046-72
- [4]. Wang Yong, Zhang Feng, Chen Xilei, Jin Yang and Zhang Jun. Burning and dripping behaviors of polymers under the UL94 vertical burning test conditions. *Fire Mater.* 34 (2010), 4, pp.203-215
- [5]. Yong Wang, Jun Zhang. Thermal stabilities of drops of burning thermoplastics under the UL 94 vertical test conditions, *J. Hazard. Mater.* (2013), 246-247, pp.103-109
- [6]. Wang Yong, Jow, Jinder, Su Kenny, Zhang Jun. Dripping behavior of burning polymers under UL94 vertical test conditions, *J. Fire Sci.* 30 (2012), 6, pp. 477-501
- [7]. Yong Wang, Jinder Jow, Kenny Su, Jun Zhang. Development of the unsteady upward fire model to simulate polymer burning under UL94 vertical test conditions. *Fire Safety J.* 54 (2012), 8, pp. 1-13
- [8]. Ezgi S.Oztekin, Sean B. Crowley, Richard E. Lyon, Stanislav I. Stolarov, Parina Patel, T. Richard Hull, Sources of variability in fire test data: A case study on poly(aryl ether ether ketone) (PEEK), *Combust. Flame*, 159 (2012), 4, pp.1720-1731
- [9]. Xuegui Wang, Xudong Cheng, Liming Li, Siuming Lo, Heping Zhang. Effect of ignition condition on typical polymer's melt flow flammability, *J. Hazard. Mater.* 190 (2011), 1-3, pp. 766-771
- [10]. Mamourian, M., Esfahani, J.A., Ayani, M.B., Experimental and scale up study of the flame spread over the PMMA sheets, *Thermal Science* 13 (1), pp. 79-88, 2009
- [11]. Ayani, M.B., Esfahani, J.A., Sousa, A.C.M., The effect of surface regression on the downward flame spread over a solid fuel in a quiescent ambient, *Thermal Science* 11 (2), pp. 67-86, 2007
- [12]. Esfahani, J.A., Abdolabadi, A.G., effect of char layer on transient thermal oxidative degradation of polyethylen, *Thermal Science* 11 (2), pp. 23-36, 2007

- [13]. Xie Qiyuan, Zhang Heping, Ye Ruibo, Experimental Study on Melting and Flowing Behavior of Thermoplastics Combustion Based on a New Setup with a T-shape Trough, *J. Hazard. Mater.* 166 (2009), 2-3, pp. 1321-1325
- [14]. Xie Qiyuan, Zhang Heping, Xu Liang. Large Scale Experimental Study on Combustion Behavior of thermoplastics with Different Thickness, *J. Thermoplast. Compos. Mater.*, 22 (2009), 5, pp. 443-451
- [15]. Kandola B.K., Price D., Milnes G.J., Da Silva A. Development of a novel experimental technique for quantitative study of melt dripping of themoplastic polymers, *Polym. Degrad. Stabil.*, 98 (2013) , 1, pp.52-63
- [16]. Q Xu, Cong Jin, Greg Griffin, Yong Jiang. Fire Safety Evaluation of Expanded Polystyrene Foam by Multi-scale Methods. *J Therm Anal Calorim*, 115 (2014), 2, pp.1651-1660.
- [17]. Smart Gillian, Kandola Baljinder K., Horrocks A. Richard, Nazare Shonali, Marney Donavan. Polypropylene fibers containing dispersed clays having improved fire performance. Part II: Characterization of fibers and fabrics from PP-nanoclay blends. *Polym. Adv. Tech.*, 19 (2008), 6, pp. 658-670
- [18]. Jozef Martinka, Tomas Chhrebet, Karol Balog. An assessment of petrol fire risk by oxygen consumption calorimetry. Published online 18 Mar. 2014, *J Therm Anal Calorim*.
- [19]. Xu Q, Griffin GJ, Burch I, Jiang Y, Preston C, Bicknel AD, Bradbury GP, White N. Predicting the time to flashover for GRP panels based on cone calorimeter test results, *J. Therm.Anal. Calorim.*, :91 (2008),3, pp:759-762.
- [20]. Przemyslaw Rybinski, Grazyna Janowska, Malgorzata Jozwiak, Marek Jozwiak. Thermal stability and flammability of styrene-butadiene rubber (SBR) composites. *J Therm Anal Calorim*. 113 (2013), 1, pp.43-52.
- [21]. Lindholm Johan, Brink Anders, Hupa Mikko. Influence of decreased sample size on cone calorimeter results, *Fire Mater*. 36 (2012), 1, pp. 63-73.
- [22]. Gregory J. Griffin, Ashley D. Bicknell, Glenn P. Bradbury, Nathan White. Effect of Construction Method on the Fire Behavior of Sandwich Panels with Expanded Polystyrene Cores in Room Fire Tests, *J. Fire Sci*. 24 (2006), 2, pp. 275-294.
- [23]. B. A. L. Östman and L. D. Tsantaridis. Correlation between cone calorimeter data and time to flashover in the room fire test, *Fire Mater*. 18 (1994), 4, pp. 205-209
- [24]. H. Hansen and P. J. Hovde. Prediction of Time to Flashover in the ISO 9705 Room Corner Test based on Cone Calorimeter Test Results, *Fire Mater*. 26 (2002), 2, pp.77-86